19th International Symposium of Ballistics, 7–11 May 2001, Interlaken, Switzerland

NUMERICAL SIMULATIONS OF DYNAMIC X-RAY IMAGING EXPERIMENTS OF 7.62-MM APM2 PROJECTILES PENETRATING B_4C

Charles E. Anderson, Jr.[1] and William A. Gooch[2]

[1] *Southwest Research Institute, P. O. Drawer 28510, San Antonio, Texas 78228 USA*
[2] *U. S. Army Research Laboratory, Aberdeen Proving Ground, MD 21005 USA*

A modification of Wilkins computational ceramics model is used to simulate experiments of the impact of the APM2 bullet and modified bullets (core and Pb nose, and core only) against B_4C targets. The experiments were conducted in the reverse ballistics mode. Flash radiography provides time-resolved penetration histories. The simulation results are compared to the experimental data; generally, agreement is very good.

INTRODUCTION

The classic study of Wilkins and coworkers in 1967–1969 [1–2] provided the first high speed photographic images and X-ray shadowgraphs (3 channels of 600 KeV) of small arms projectiles impacting ceramic targets. Wilkins used a monolithic hard steel (R_c55) projectile as a surrogate projectile for the 7.62-mm armor-piercing (AP) bullet. Wilkins also developed a phenomenological computational ceramics model for thin tiles and compared the results of numerical simulations – using the Lagrangian hydrocode HEMP – with experiments. He then performed parametric studies to investigate the influence of ceramic material properties on ballistic performance [1–2].

The 7.62-mm APM2 bullet is exceedingly more complex than the monolithic surrogate used by Wilkins. A schematic of the bullet is shown in Fig. 1. The bullet consists of a jacket made of gilding metal (90% Cu, 10% Zn), 4.21 g; a lead (Pb) nose element, 0.78 g; a Pb base filler, 0.50 g; and a very hard steel core, 5.25 g. The lead nose is pressed over the steel core and both are encased in the metal jacket. The masses are nominal values. Some lots of bullets do not contain the Pb base filler, and then the Pb point filler is slightly more massive (e.g., 1.3 g), with the total mass of the bullet still 10.6–10.7 g. The core design dates from 1939; the 1070 tool steel core has a classical ogive nose and boat tail design; the core is very hard, measuring Rockwell C62–65.

The U. S. Army Research Laboratory (ARL) adapted dual one-MeV X-ray pulsers to obtain two shadowgraph images of the impact of the APM2 bullet impacting boron carbid (B_4C) [3–4]. The goal was to conduct a high fidelity diagnostic analysis of penetrator/bullet interaction during the first 55 μs after impact. Three conditions of the projectile were tested: the full metal jacket (FMJ) projectile; the lead (Pb) tip and steel core only; and just the steel core. The FMJ was removed by machining for tests with the core, or nose and core only. These conditions allow the separation of the ballistic contributions of the projectile components. A flash X-ray shadowgraph of each projectile is shown in Fig. 2.

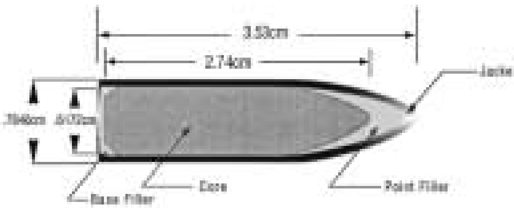

Figure 1. Schematic of 7.62-mm APM2 bullet.

Figure 2. Static X-rays of projectiles.

Numerical simulations using the Johnson-Holmquist ceramics constitutive model for B4C [5] were not in good agreement with the experiments [3]. The authors report that the most obvious discrepancy was the inability of the simulations to replicate the erosion of the steel core [3]. Walker and Anderson [6] took Wilkins' computational ceramics model and implemented the model into CTH [7]. The model was applied to Al_2O_3 ceramic tiles and the M80 ball round. Later, the model was applied to B_4C ceramic tiles impacted by Wilkins surrogate AP bullet, and modifications were required in order for the simulations to match experiment [8]. This modified model is now usod to simulate the reverse ballistic experiments for the three projectiles shown in Fig. 2.

A brief description of the experiments will be given, followed by a summary of the modifications made to the Wilkins ceramic model. Then the simulation results will be compared to the experimental data.

EXPERIMENTAL SETUP AND RESULTS

The experiments consisted of 8.2-mm-thick B_4C, 76 mm in diameter, backed by a 38.1-mm polyethylene, all encased in a polypropylux plastic sabot. The B_4C tiles were hot-pressed by Cercom, Inc., of Vista, CA, and had a density of 2.51 g/cm^3. The package was fired from a 100-mm diameter light gas gun. The experiments were performed in the reverse ballistics mode where the "target" was fired at the stationary bullet, shown in Fig. 3. The impact velocity varied between 856 m/s and 860 m/s. Other details about the experiments are described in Refs. [3–4].

A time delay circuit was used to set the delay between the two X-rays to 10 µs. The flash X-ray images were enhanced digitally, and a set of physical measurements were

Home
Table of Contents

taken from the X-ray film as defined in Fig. 4. Time is measured from impact. The experimental results are summarized in Ref. [3–4].

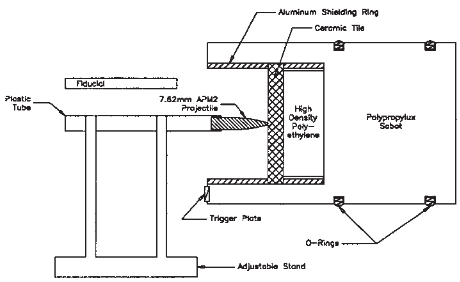

Figure 3. Reverse ballistics target assembly.

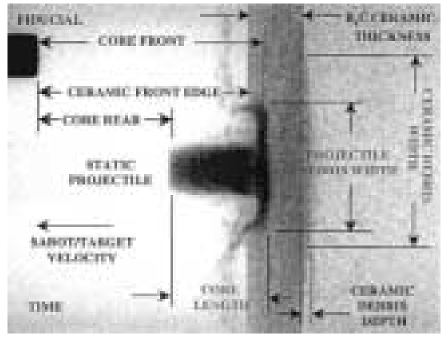

Figure 4. X-ray measurements.

NUMERICAL SIMULATIONS

Modifed Wilkins' Ceramic Constitutive Model

Anderson and Walker incorporated Wilkins' ceramic model into the Eulerian wavecode CTH [7] and compared the computational results to flash X-ray shadowgraphs taken by Wilkins, *et al.* [9] of the surrogate projectile impacting B_4C tiles. The simulations results did not agree with the results inferred from the X-ray images. Additionally, results from numerical simulations using the Wilkins model did not agree with experimental data for the APM2 bullet [10]. To understand the discrepancies necessitated a re-examination of the model [8]. Two very important modifications were required for the model to replicate experimental observations. First, it was found that a description of the shear strength of the failed ceramic material is necessary. A Drucker-Prager model was incorporated into the overall ceramics model to account for the strength of failed ceramic.

The second modification is associated with the speed of damage. The original model assumed that the transition of strength from intact to failed ceramic was associated with crack propagation. It was found that damage propagation had to be slowed significantly – by approximately a factor of 20 relative to a crack propagation velocity – for the simulations to replicate experimental details. Within the context of the model, a damage variable controls the maximum speed of damage propagation. It appears that there are two distinct phenomena concerning the impact and penetration of a ceramic tile. First, there is the appearance of cracks. Radial cracks appear first, the result of hoop tensile stresses, followed by circumferential cracks, forming fracture conoids. Although these cracks certainly degrade the structural integrity of the ceramic, large pieces of ceramic remain in the path of the projectile. To penetrate, the projectile must "grind up" the ceramic – called comminution – into a very fine ceramic "powder." This comminuted material is referred to as the Mescall zone [11]. It is this comminution process that dominates the penetration dynamics of ceramic tiles [8]. With these modifications, simulations reproduce the ballistic limit experiments of Wilkins for boron carbide on an aluminum substrate [8].

Simulations of Experiments

It was reported in Ref. [3] that numerical simulations could not replicate erosion of the steel core. The fundamental cause of for this failure to reproduce the experimental results is a consequence of the inability of the ceramics constitutive model to capture the phenomenon called *dwell*, where the impacting projectile “sits” on the ceramic front face and does not penetrate the ceramic. During dwell, the projectile loses kinetic energy due to both mass loss and deceleration.

We use the ceramic model of Wilkins as modified by Walker and Anderson [6,8] to simulate the experiments described in Refs. [3–4]. The simulations are presented in the order of increasing complexity of the projectile, i.e., the core only; the Pb nose and core, and the FMJ projectile. All simulations were conducted for an impact velocity of 857.8 m/s, an average of the experimental impact velocities. For purposes of the simulations, “0” denotes the target surface – and the tip of the projectile – at the time of impact (taken as $t = 0$).

The positions of the nose and tail of the core are plotted as the solid symbols versus time in Fig. 5(a). Although there was not a flash X-ray shadowgraph at $t = 0$, the positions of the nose and tail, as well as the length of the projectile, can be plotted because of pretest measurements. Evidence for dwell is seen in the experiments as well as in the simulations. There is little to no penetration for the first 15 µs, and only 3 mm of penetration at 25 µs. However, with failure of the ceramic, the penetration rate increases. The simulation result passes through the first two experimental data points for the tail position, but overestimates the tail position for the next two data points. The simulation result for the tail position agrees better with the last two experimental data points. This will be discussed further in the paragraphs below. It appears that the simulation slightly overpredicts the depth of penetration into the target.

We make a distinction between comparisons of nose/tail positions and the length of the core. Nose and tail positions were measured relative to a fiducial system, as was the front surface of the ceramic. These data were then used to calculate the positions of the nose and tail relative to the impact surface. The position of the impact surface is difficult to measure precisely since the image on the flash radiograph is a “shadow” of the ceramic tile projected onto a plane. Any error associated with ascertaining the location of the impact surface results in errors for the nose and tail positions. In contrast, projectile length is measured directly from the radiographs.

In general, numerical simulations fairly accurately predict the position of the projectile tail versus time since this is primary kinematics. The simulation result passes through the experimental values at 15 µs and 25 µs in Fig. 5(a). The simulation result is above the data points at 25 and 35 µs, implying that the tail is moving faster in the simulation than in the experiment. However, the two data points at 45 and 55 µs are close to or on the simulation result. Thus, the experimental data, taken at face value, would indicate that the tail velocity accelerated between 35 and 45 µs.[1] Clearly, the projectile tail does not speed up during penetration (the simulation result shows that the tail position vs. time is concave down, indicating that the tail is decelerating). Thus, it is concluded that one or more of the

1 It is noted that the impact velocity for these data points differed only by 3 m/s, so different impact velocities cannot be the source of the discrepancy.

position measurements is in error; and from the preceding discussion, it is most likely that there is some error in determining the location of the original impact surface. If it is assumed that the simulation result is reasonably accurate for the position of the tail vs. time, then the experimental tail data can be shifted to lay on the simulation results.[2] The nose position needs to be displaced the same distance since it also is plotted relative to the impact surface. The open circles in Fig. 5(a) denote this shift. Except for the nose position at 55 µs, where the X-ray shadowgraph shows a fractured core, the simulation result is in good agreement with the experimental results.

The experimentally measured core lengths versus time are plotted as the solid symbols in Fig. 5(b). The error bars indicate approximately ± 1 mm uncertainty in the measurements. The solid line represents the simulation result. The core fractured longitudinally and split along the centerline, resulting in a “false” length, for the data point at 57 µs. Agreement, in general, is quite good. The fact that the core length is reproduced reasonably well supports our argument for the position errors for Fig. 5(a).

The dashed line in Fig. 5(b) represents the simulation result for the Pb-nose-plus-core projectile. The open symbols denote the experimentally measured lengths for this projectile. The Pb-core projectile should have an initial length of 3.2 cm; however, in the process of removing the jacket, some lead was inadvertently removed. A picture of one of the projectiles actually shows the tip of the core just visible in front of the Pb element. Thus, the Pb-core projectiles do not have lengths as might be supposed; instead, the lengths are between that of the core-only and Pb-core projectile. Therefore, the experimental results – the open circles in Fig. 5(b) – should fall between the core only data and the theoretical response of the Pb-core projectile. This is exactly the case, although the results tend to be closer to the core-only projectile. This is reasonable since the process of removing the jacket almost surely removes some of the Pb material at the tip of the bullet nose. The dotted line is the calculated length of the core for the Pb-core projectile. The simulation predicts that the Pb nose damages the ceramic, with the subsequent effect that a somewhat longer steel core (~ 5 mm) remains after penetrating the ceramic tile; this has been observed experimentally [10].

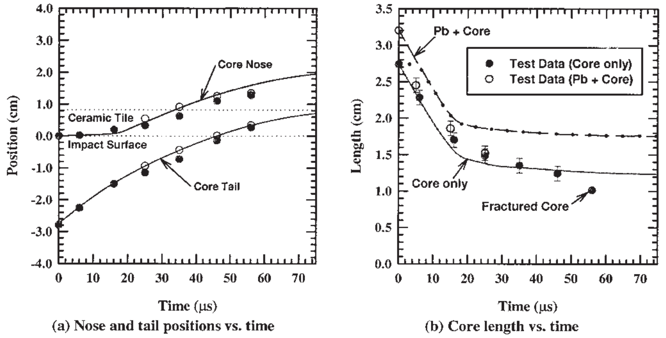

Figure 5. (a) Position-time history of the nose and tail and (b) steel core length vs. time for the core-only and Pb-nose+core projectile.

2 This corresponds to an error of only a few millimeters in determining the position of the front face of the ceramic.

The simulation and experimental data for the FMJ projectile are compared in Fig. 6. The solid lines in Fig. 6(a) represent the positions of the nose and tail of the FMJ projectile, while the dotted lines denote the positions of the tip and tail of the core. The tip of the core reaches the projectile-target interface at approximately 8 µs after impact, and from that time on, the nose of the eroded projectile and the nose of the core are coincident. The solid triangles denote the experimental data. Although flash radiographs exist at 7 and 17 µs, absolute positions could not be determined.

If it is again assumed that there is a slight error in determining the absolute position of the front surface of the ceramic tile, and that the experimental and calculated tail positions should coincide, then the experimental data can be shifted as was done in Fig. 5; the shifted data are denoted by the opened triangles. Again, the simulations are in good agreement with the experimental results.

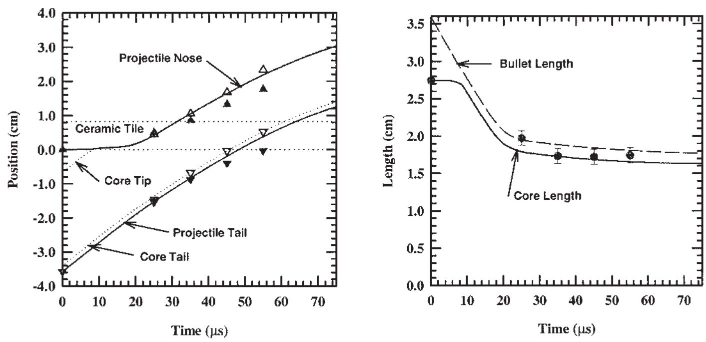

(a) Nose and tail positions vs. time
(b) Core length vs. time

Figure 6. (a) Position-time history of the nose and tail and (b) FMJ length and steel core length vs. time for the FMJ projectile.

The total bullet length and the core length versus time are plotted as the dashed and solid lines in Fig. 6(b), respectively. The solid symbols denote the experimental data. The measured length at 25 µs agrees with the calculated length for the total projectile, but the lengths at later times agree better with the calculated length for the core. This is consistent with the flash radiographs, as shown in Fig. 7. At 35 µs, the jacket is sliding past the core. The core, because it has a strength approximately double that of the jacket, is decelerated faster than the jacket. The measurements from the flash radiographs are to the tail of the core. In the simulation, however, the core and the jacket remain together and do not separate.

CONCLUSIONS

Numerical computations were conducted to simulate reverse ballistic experiments to examine the time-resolved penetration of into a boron carbide tile by three different projectiles, the 7.62-mm APM2 bullet, and two modified bullets. The ceramics model of Wilkins, as modified by Walker and Anderson, was used to represent the constitutive response of the ceramic. The simulations reproduce the phenomenon of dwell, and for the most part, show very good agreement with the experimental data. The simulations agree very well with the projectile lengths measured from the flash radiographs. The positions of the projectile nose and tail relative to the ceramic front surface are in good agreement after a slight adjustment to the "apparent" position of the ceramic surface. One discrepancy is noted between the simulations and experiments. In the experiments, the core is decelerated faster than the jacket, and the jacket slides down over the core. This observation is not reproduced in the simulations.

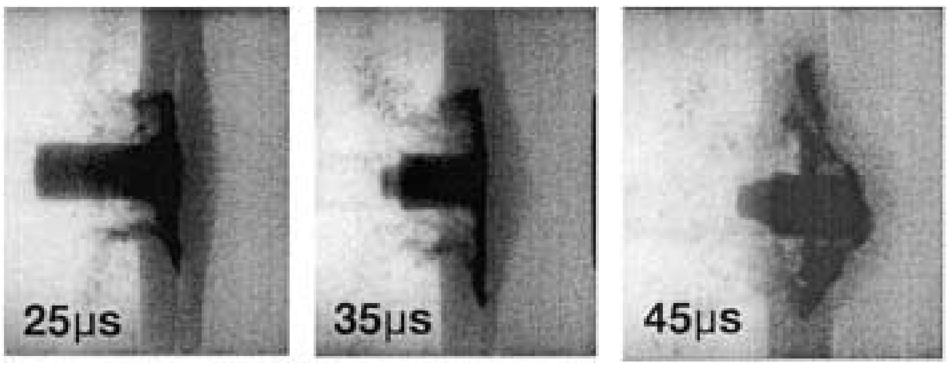

Figure 7. Flash radiographs of the FMJ projectile.

REFERENCES

1. M. L. Wilkins, "Third Progress Report of Light Armor Program," UCRL-50460, Lawrence Livermore Laboratory, Livermore, CA, July 1968.
2. M. L. Wilkins, "Mechanics of penetration and perforation," *Int. J. Engng. Sci.*, **16**(11), 793–807 (1978).
3. W. A. Gooch, M. S. Burkins, P. Kingman, G. Hauver, P. Netherwood, and R Benck, "Dynamic X-Ray Imaging of 7.62-mm APM2 Projectiles Penetrating Boron Carbide," *18th Int. Symp. on Ballistics*, Vol. 2, 901–908, Technomic Publishing Company, Inc., Lancaster, PA, 1999.
4. W. A. Gooch, M. S. Burkins, G. Hanver, P. Netherwood, and R. Benck, "Dynamic X-rays imaging of the penetration of boron carbide," *J. Phys. IV France,* **10**, Pr9-593-588, 2000.
5. G. R. Johnson and T. J. Holmquist, "Response of Boron Carbide Subjected to Large Strains, High Strain Rates, and High Pressures," *J. Appl. Phys.*, **85**(12), 8060–8073, 1999.
6. J. D. Walker, C. E. Anderson, Jr., and P. A. Cox, "Computational Modeling of Thin AD-85 Ceramic Tiles Backed by Thin Aluminum Substrates," *15th Int. Symp. on Ballistics,* Vol. 1, pp. 395–402, Jerusalem, Israel, May 21–24, 1995.
7. J. M. McGlaun, S. L. Thompson, and M. G. Elrick, "CTH: A Three-Dimensional Shock Wave Physics Code," *Int. J. Impact Engng.,* **10**, 351–360, 1990.
8. C. E. Anderson, Jr. and J. D. Walker, "Ceramic Dwell and Defeat of the 0.30-Cal AP Projectile," *15th U.S. Army Symp. on Solid Mech.*, Myrtle Beach, SC, April 12–14, 1999.
9. M. L. Wilkins, R. L. Landingham, and C. A. Honodel, "Fifth Progress Report of Light Armor Program," UCRL-50980, Lawrence Livermore Laboratory, Livermore, CA, 1970.
10. C. E. Anderson, Jr., unpublished data, 1999.
11. D. A. Shockey, A. H. Marchand, S. R. Skaggs, G. E. Cort, M. W. Burkett, R. Parker, "Failure Phenomenology of Confined Ceramic Targets and Impacting Rods", *Int. J. Impact Engng.*, **9**(3), 263–275, 1990